

Original Article

Toxicity assessment and bioimaging potential of carbon dots synthesized from banana peel in zebrafish model

Ni PAD. Wijayanti¹, Fitri A. Permatasari^{2,3,4}, Sophi Damayanti^{5,6}, Kusnandar Anggadiredja⁷, Fery Iskandar^{2,3,4}, Indra Wibowo⁸ and Heni Rachmawati^{1,3*}

¹Research Group of Pharmaceutics, School of Pharmacy, Institut Teknologi Bandung, Bandung, Indonesia; ²Department of Physics, Faculty of Mathematics and Natural Sciences, Institut Teknologi Bandung, Bandung, Indonesia; ³Research Center for Nanosciences and Nanotechnology, Institut Teknologi Bandung, Bandung, Indonesia; ⁴Collaboration Research Center for Advanced Energy Materials, National Research and Innovation Agency, Institut Teknologi Bandung, Bandung, Indonesia; ⁵Research Group of Pharmacochimistry, School of Pharmacy, Institut Teknologi Bandung, Bandung, Indonesia; ⁶Department of Natural Language Processing and Big Data Analysis, Center of Excellence on Artificial Intelligence for Vision, Institut Teknologi Bandung, Bandung, Indonesia; ⁷Department of Pharmacology and Clinical Pharmacy, School of Pharmacy, Institut Teknologi Bandung, Bandung, Indonesia; ⁸Department of Physiology, Animal Development and Biomedical Science Research Group, School of Life Sciences and Technology, Institut Teknologi Bandung, Bandung, Indonesia

*Corresponding Author: h_rachmawati@itb.ac.id

Abstract

Zebrafish serve as a pivotal model for bioimaging and toxicity assessments; however, the toxicity of banana peel-derived carbon dots in zebrafish has not been previously reported. The aim of this study was to assess the toxicity of carbon dots derived from banana peel in zebrafish, focusing on two types prepared through hydrothermal and pyrolysis methods. Banana peels were synthesized using hydrothermal and pyrolysis techniques and then compared for characteristics, bioimaging ability, and toxicity in zebrafish as an animal model. Pyrolysis-derived banana peel and hydrothermal-derived banana peel showed blue emission under ultraviolet light, indicating excitation-dependent behavior. To test their potential application for bioimaging, a soaking method was used using zebrafish that showed fluorescence intensity in the eyes, abdomen, and tail of zebrafish. Toxicity comparison showed that pyrolysis-derived banana peel had lower toxicity with 50% lethal concentrations (LC₅₀) of 1707.3 ppm than hydrothermal-derived banana peel (LC₅₀ 993 ppm) in zebrafish. Both types of carbon dots showed significant differences ($p < 0.05$) in hatching rates at 96 and 120 hours of exposure. Of the two methods for carbon dot synthesis from banana peel, the pyrolysis method had a higher toxicity threshold than the hydrothermal method, as indicated by the LC₅₀ value and the number of zebrafish embryos that died, hatched delayed, and experienced malformation during their development.

Keywords: Carbon dots, pyrolysis, hydrothermal, LC₅₀, zebrafish

Introduction

Nanomaterials are increasingly vital in healthcare, particularly in medical imaging, disease diagnosis, and vaccine development [1-3]. Carbon-based nanomaterials, especially carbon dots, exhibit promising potential due to their high biocompatibility, visibility, light stability, minimal toxicity, and unique optical properties [4-6]. Carbon dots are widely utilized in nanomedicine, notably in drug delivery, bioimaging, and diagnostics [7-12]. Functionalization of carbon dots with biomolecules, such as antibodies and folic acid, enhances targeting and delivery efficiency [13]. Carbon dots have demonstrated improved efficacy and reduced toxicity in delivering drugs such as doxorubicin, curcumin, and 5-fluorouracil, a pH-responsive drug for cancer therapy [14-



17]. In bioimaging and diagnostics, carbon dots provide superior brightness, biocompatibility, and photostability [7-11,18,19], enabling their use in cellular imaging, tissue visualization, and the detection of biomolecules and pathogens in biosensors [12,20].

Carbon dots are nanoparticles synthesized through various methods, including top-down and bottom-up approaches [21-23]. While chemical precursors are commonly used, there is increasing interest in eco-friendly and sustainable alternatives [24,25]. Natural precursors, such as biomass, food waste, and biofluids, offer a promising option due to their renewability, low cost, environmental friendliness, and superior biocompatibility [18,26,27]. Carbon dots derived from these sources are particularly suited for biomedical applications owing to their excellent biocompatibility [18,28-32]. In assessing biocompatibility, toxicity evaluation is crucial, with zebrafish (*Danio rerio*) emerging as a popular in vivo model due to its small size, optical clarity, low maintenance cost, and genomic similarity to humans [33-36]. Zebrafish are easily bred, have a short embryonic development period, and share over 70% of human genes, enabling rapid and reliable toxicity assessments [37-39]. Additionally, zebrafish have been utilized in various biomedical assessments, including gene therapy and bioimaging [34,40-46].

Numerous studies have utilized zebrafish for toxicity and bioimaging assessments [7,8,35,43,45,47-53]. Dias *et al.* conducted a nanotoxicity evaluation of carbon dots derived from kiwi, avocado, and pear, synthesized via the hydrothermal method, using zebrafish [47]. The 50% lethal concentrations (LC₅₀) for kiwi, avocado, and pear-derived carbon dots were 1444, 1964, and 2224 ppm, respectively, categorizing them as non-toxic in zebrafish and suitable for potential bioimaging applications [47].

Carbon dots synthesized from banana peel have shown promise in bioimaging, antibacterial activity, and biosensing [18,26,28,54-56]; however, their toxicity in zebrafish has not been studied. To the best of our knowledge, no toxicity assessments of banana peel-derived carbon dots using zebrafish have been reported. Although carbon dots are generally considered safe for biological systems, further research is necessary to fully evaluate potential risks before widespread application [45]. Therefore, investigating the effects of these carbon dots on cells and organs is crucial, as current knowledge remains limited.

The aim of this study was to assess the toxicity of carbon dots derived from banana peel in zebrafish, focusing on two types of preparations: through hydrothermal and pyrolysis methods. The potential application of these carbon dots as bioimaging agents was also evaluated. The findings highlight the advantages of green synthesis methods in producing carbon dots with reduced environmental impact and low toxicity, suggesting potential applications in pharmaceutical sciences.

Methods

Study design and setting

Banana peels were synthesized into carbon dots using two types of synthesis methods: pyrolysis and hydrothermal. The carbon dots were then characterized physicochemically, including morphology and particle size, surface charge, optical properties, and functional group characterization. Carbon dots that have been characterized were then tested for biodistribution and toxicity in zebrafish embryos and larvae using the soaking method. A total of 20 embryos and larvae were used for bioimaging testing, and 140 embryos (12 hours post-fertilization (hpf)) were used for toxicity testing, with 20 embryos per concentration of carbon dot solution. Embryos were randomly selected with inclusion criteria including fertile and healthy embryos aged 12 hpf, while exclusion criteria included infertile embryos and embryos that did not develop.

Sampling strategy and criteria

The samples used in toxicity testing were zebrafish embryos aged 12 hpf, with the inclusion criteria being healthy fertile embryos aged 12 hpf. Healthy fertile embryos had spherical characteristics with a transparent interior. The exclusion criteria were infertile embryos and those not spherical in shape. The embryos were observed under a stereo microscope, randomly selected by blinded researchers from all embryos produced through zebrafish mating. The embryos were then randomly grouped and placed in a wellplate, containing five embryos per plate. The number of embryos used was 20 for each concentration of carbon dots solution; therefore, the total

embryos used were 140 embryos for seven concentrations of carbon dots tested. The number of embryos used and the toxicity testing procedures were in accordance with OECD guidelines [57].

Zebrafish embryos that had been grouped in well plates were treated by soaking them in 2 mL of different medium for 120 h and observed every 24 hours. The treatments given consisted of the control group which was soaked with E3 culture medium (0 ppm carbon dots solution) in a wellplate. The treatment groups 1 to 5 were soaked with carbon dots solution in E3 culture medium with varying concentrations: 125, 250, 500, 1000, and 2000 ppm. The positive control group was soaked in a 3,4 dichloroaniline solution.

Banana peels preparation

Banana peels (*Musa paradisiaca* L.) used in this study were sourced from the Jimbaran food market in Badung, Bali, Indonesia, and were botanically identified by the Indonesia National Research and Innovation Agency (BRIN). Bananas were separated from their skin and pulp, then washed and cut into small pieces to be used as materials in the synthesis of carbon dots.

Synthesis of carbon dots via pyrolysis and hydrothermal methods

For the pyrolysis method, 15 g of banana peel were ground, mixed with 100 mL of deionized water, and heated at 300°C for 30 min in a furnace, producing 5.90 g of black powder containing carbon dots (**Figure 1**). To synthesize the carbon dots through the hydrothermal method, 15 g of banana peel were finely ground, combined with 100 mL of deionized water, placed in a Teflon-lined autoclave, and heated at 135°C for 24 hours. After cooling to ambient temperature, the solution was filtered through a 0.22 µm syringe filter. The resulting brownish-yellow solution was vacuum freeze-dried (Labconco, Tokyo, Japan) for 48 hours to obtain a 0.14 g solid brown powder of carbon dots (**Figure 1**).

Size and morphological analysis

The size and morphology of the carbon dots were analyzed using a transmission electron microscope (TEM) (Hitachi HT7700, Tokyo, Japan). The TEM grids were prepared by placing carbon-coated copper grids into the carbon dot solution, air-dried, and then imaged at 120 kV. Particle diameters, approximately 100 particles, were measured using ImageJ software (National Institutes of Health and Laboratory for Optical and Computational Instrumentation, University of Wisconsin, United States).

Optical characteristics

The absorbance of the carbon dots was measured using a UV-Vis spectrophotometer (Shimadzu UV-1800, Tokyo, Japan) with a wavelength range of 200–800 nm, while the emission and excitation spectra were analyzed with a fluorescence spectrophotometer (Agilent Technologies, Inc., Santa Clara, California, USA) using 5 nm excitation and 5 nm emission slit widths. The fluorescence behavior was then evaluated by varying the excitation wavelength from 300 to 700 nm at 25 nm intervals (**Figure 1**).

Characterization of functional groups and surface charge measurement

Functional groups of the carbon dots were characterized using a Fourier transform infrared (FTIR) spectrophotometer (Shimadzu IRPrestige-21, Tokyo, Japan), with the sample incorporated into a KBr pellet and analyzed in the 4000–500 cm⁻¹ range. After obtaining the absorbance values at the peaks of the FTIR spectra of the two carbon dots, the absorbance values were compared with the standard library, which showed the absorption in the functional group area. The surface charge of the carbon dots was determined using zeta potential analysis (Horiba SZ-100, Tokyo, Japan) by placing 1 mL of the sample in the zeta cell, with measurements replicated three times.

Zebrafish embryo husbandry and breeding

Forty to fifty adult zebrafish (0.4–0.6 grams; 4–5 months old), were obtained from a breeder based in Bogor, West Java, Indonesia, and were kept in 12 L tanks with a recirculating aquaculture system, maintained at 28°C with a 14:10 h light-dark cycle. A continuous water flow was provided. Zebrafish were fed commercial pellets three times daily. Adult zebrafish in a 2:1 male-to-female ratio were selected for breeding in a separate tank with a fish net to prevent egg consumption.

Spawning occurred upon exposure to light, and eggs were harvested at 4–5 hpf and analyzed under a stereo microscope Axiocam 208 Color (Zeiss, Oberkochen, Germany) at 1.575× magnification. The eggs were categorized as fertilized or unfertilized based on their visual appearance. Fertilized eggs were placed in 24-well plates with 2 mL of E3 medium and five embryos per well.

Carbon dot fluorescence distribution in zebrafish embryos and larvae

Zebrafish embryos and larvae (6 hpf and 84 hpf) were soaked in 2 mL of E3 medium containing 125 ppm of banana peel carbon dots for 4 h in a 24-well cell-culture plate, with five embryos and larvae per well; a total of 20 embryos and larvae were used for this test. The embryos were cultured at 28°C with a 14:10 h light-dark cycle. After 4 h of soaking, the embryos were washed with E3 medium to remove residual carbon dots. Fluorescence images were captured using a confocal microscope (Olympus Fluoview FV1200, Tokyo, Japan) at wavelengths of 488 nm (green) and 405 nm (blue) (**Figure 1**).

Acute toxicity assessment of carbon dots in zebrafish embryos

Acute toxicity of fertilized zebrafish embryos (12 hpf) was assessed following the OECD Fish Embryo Acute Toxicity Test guideline (Test No. 236), with minor modifications [57]. Zebrafish embryos were exposed to banana peel-derived carbon dots (0, 125, 250, 500, 1000, and 2000 ppm) for 120 h. Culture medium was used as the negative control, and 3,4-dichloroaniline served as the positive control. Five embryos were placed in each well of a 24-well plate, with 2 mL of the respective carbon dot solutions. Survival rates, malformations, and hatching rates were evaluated every 24 h by comparing the number of live embryos or hatched eggs in the experimental group to the control group under a stereo microscope (magnification 1.575×), with experiments replicated three times [37]. Embryo mortality was assessed based on four indicators: failure to develop body segments, absence of heartbeat, abnormal tail development, and egg coagulation [33,37]. The LC_{50} value was calculated using probit analysis by entering the number of fish that die at each concentration of carbon dots solution in the Excel probit analysis program; then the program calculated the LC_{50} value using a linear regression equation [58]. Embryos showing malformations or delayed hatching were observed under a stereo microscope and were euthanized by immersion in 100 ppm clove oil for 45–50 minutes [59–61] (**Figure 1**).

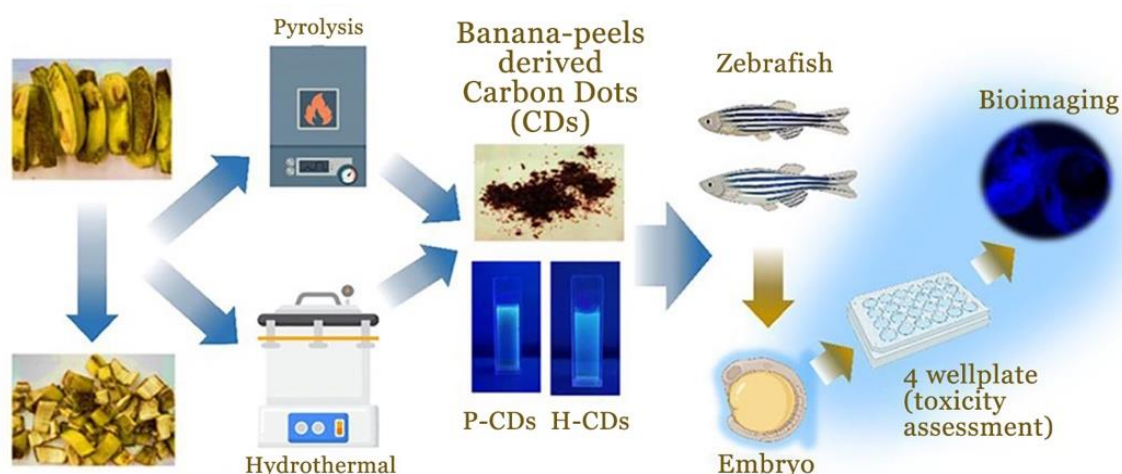


Figure 1. Schematic illustration of fluorescent carbon dot preparation via pyrolysis and hydrothermal methods, along with toxicity and bioimaging assessments in zebrafish.

Study variables

The independent variable in this study was the concentration of carbon dots solution (0, 125, 250, 500, 1000, and 2000 ppm) used in the soaking method, while the dependent variables were the intensity of fluorescence qualitatively in the biodistribution test and the number of dead zebrafish and zebrafish embryos that were delayed in hatching and malformations that occurred during the development of zebrafish for 120 h. The fluorescence intensity of carbon dots was visually assessed using confocal microscopy in the eyes, abdomen and tail of larvae, as well as in the

chorion of zebrafish embryos. The number of dead zebrafish was counted; malformed zebrafish during development were observed under a stereo microscope, and embryos that experienced delayed hatching were compared with the developmental reference of zebrafish embryos.

Statistical analysis

Continuous data were presented as mean and standard deviation (for normally distributed data) and median (minimum-maximum) for non-normally distributed data; categorical data were presented as frequency and percentages. The Shapiro-Wilk test was utilized to assess data normality. ANOVA and Tukey tests were used to assess survival and hatching rates. Toxicity assays were analyzed using the Probit model with Weibull distribution [58]. Minitab 21.1. (Minitab LLC., Pennsylvania, USA) was employed for data analysis, with $p < 0.05$ considered statistically significant.

Results

Synthesis and characterization of carbon dots

Banana peel carbon dots synthesized via pyrolysis and hydrothermal methods exhibited distinct characteristics. Organoleptically, pyrolytic banana peel carbon dots (P-CDs) were described as a black powder with an ashy odor, whereas hydrothermal banana peel carbon dots (H-CDs) were identified as a black hygroscopic powder with a caramel odor. The surface charge of P-CDs was -49.8 ± 1.01 mV, while H-CDs exhibited a surface charge of -22.7 ± 0.67 mV. P-CDs had a smaller particle size (1.8 ± 0.4 nm) compared to H-CDs (5.4 ± 1.3 nm) (**Figure 2A** and **Figure 2B**).

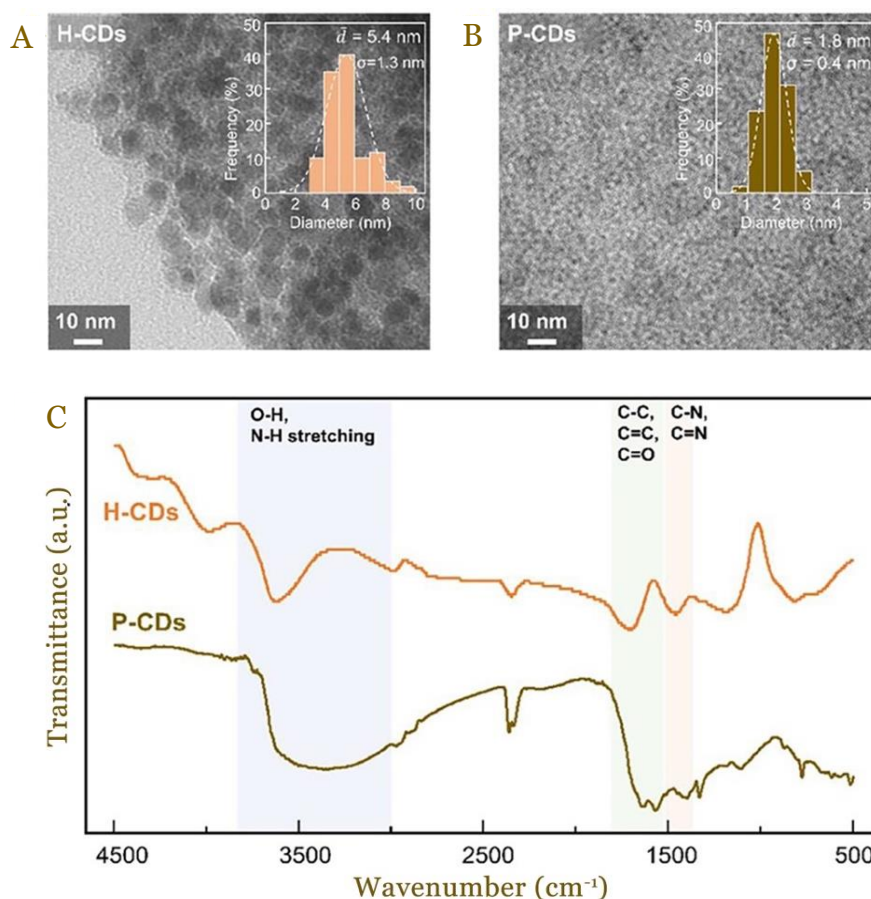


Figure 2. Molecule characteristics of synthesized pyrolytic banana peel carbon dots (P-CDs) and hydrothermal banana peel carbon dots (H-CDs). (A-B) Transmission electron microscope (TEM) images of synthesized carbon dots. The inset shows a particle size distribution graph of the carbon dots. (C) Comparison analysis of FTIR spectra between pyrolytic banana peel carbon dots (P-CDs) and hydrothermal banana peel carbon dots (H-CDs).

FTIR spectrum of P-CDs displayed a peak at 2972 cm^{-1} , corresponding to the stretching of sp^3 CH bonds (**Figure 2C**). Prominent peaks at 2360 cm^{-1} and 1566 cm^{-1} indicated the presence

of C=O bonds, while peaks at 1396 cm^{-1} and 1311 cm^{-1} signified C=N bonds. Conversely, the FTIR spectrum of H-CDs revealed an apparent peak at 3630 cm^{-1} , associated with combined hydroxyl (OH) groups (**Figure 2C**). A peak at 2978 cm^{-1} was attributed to sp^3 hybridized carbon-hydrogen (CH) bonds. Additional peaks at 2349 cm^{-1} and 1705 cm^{-1} corresponded to functional groups containing C=O bonds. These distinctive optical and physicochemical properties defined H-CDs.

The UV spectra of P-CDs and H-CDs revealed that maximum absorbance occurred between 230 and 320 nm (**Figure 3A**). The absorption of visible light, spanning 350 to 550 nm, was primarily attributed to the surface functional groups of the carbon dots, while ultraviolet light absorption in the 230 to 320 nm range was associated with electronic transitions ($\pi\text{-}\pi^*$) within the carbon core's C=C bonds. In both synthesis methods, under 365 nm UV light, the carbon dots in solution exhibited intense green fluorescence (**Figure 3B**).

The photoluminescence spectra of the carbon dots, recorded at different excitation wavelengths from 300 to 700 nm (**Figure 3B**), revealed that P-CDs exhibited the highest photoluminescence intensity with a peak emission around 471 nm when excited at 365 nm. In contrast, H-CDs showed a maximum emission peak at approximately 441 nm (**Figure 3B**). The photoluminescence intensity increased with excitation wavelengths from 300 to 365 nm but gradually decreased when the excitation wavelengths exceeded 393 nm for pyrolysis and 374 nm for hydrothermal methods. These findings indicated that the synthesis method influenced the photoluminescence intensity and emission characteristics.

An intriguing property of the banana peel carbon dots was their excitation-wavelength-dependent emission spectrum (**Figure 3C** and **Figure 3D**). As excitation wavelengths increased from 300 nm to 700 nm, the emission peaks shifted to longer wavelengths (red-shifted). Due to their fluorescent properties, banana peel carbon dots hold potential for imaging applications.

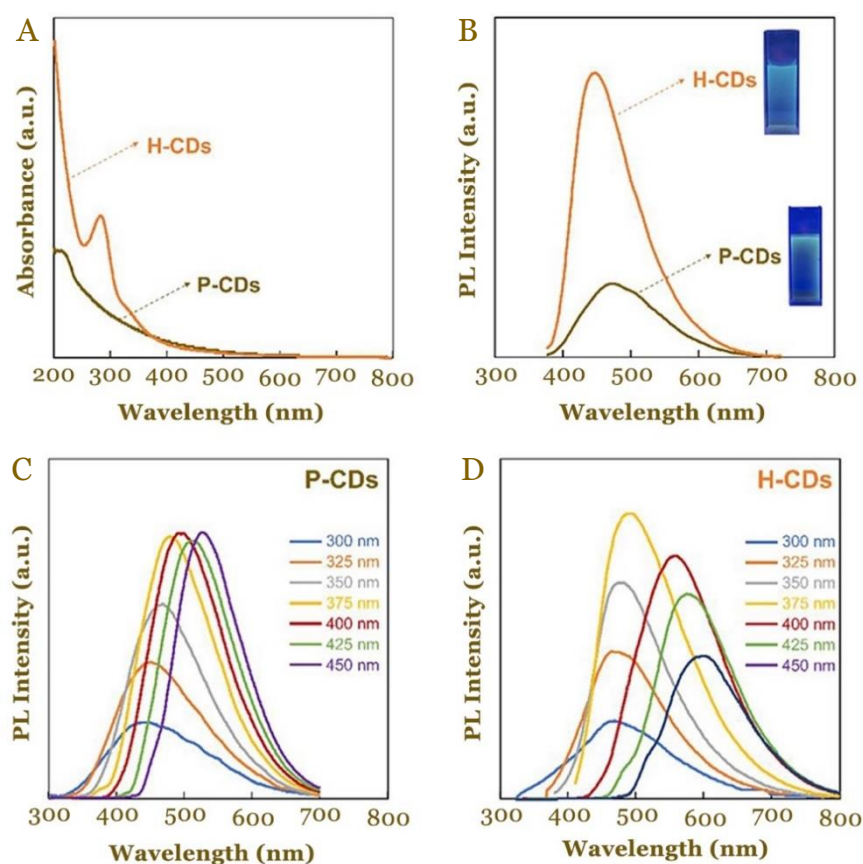


Figure 3. Optical characteristic of banana peel-derived carbon dots. (A) Comparison analysis of UV-Vis absorption spectra. (B) Comparison of fluorescence excitation spectra and optical images of banana peel carbon dots solution under UV light at 365 nm. (C) Excitation-dependent emission behavior of pyrolytic banana peel carbon dots. (D) Excitation-dependent emission behavior of hydrothermal banana peel carbon dots.

Evaluation of banana peel carbon dots distribution in zebrafish embryos and larvae model

The data revealed that the carbon dots exhibited strong fluorescence in the yolk sac, intestine, and eye lens of zebrafish embryos and larvae, but displayed weak fluorescence in the tail (**Figure 4**). In zebrafish embryos, the carbon dots were confined to the perivitelline area and did not penetrate beyond the chorion, resulting in fluorescence primarily surrounding the embryo (**Figure 4A**).

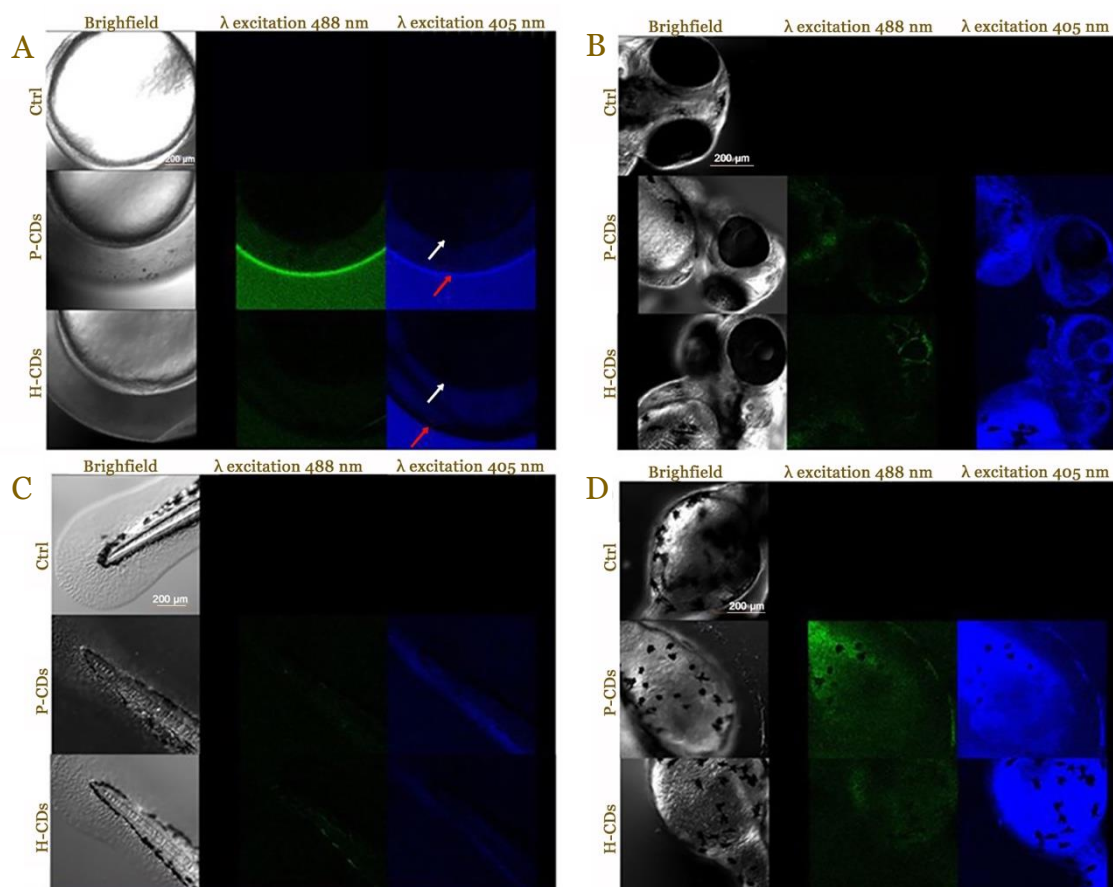


Figure 4. Distribution of banana peel carbon dots on zebrafish embryos and 84 hours post-fertilization (hpf) larvae after treatment with 125 ppm of carbon dots. Brightfield and fluorescence images of zebrafish embryos after 4 hours of exposure. (A) 6 hpf zebrafish embryos. (B) Head, eye, and lens of 84 hpf zebrafish. (C) Tail of 84 hpf zebrafish. (D) Yolk sac and intestine of 84 hpf zebrafish. Observations were made using a confocal microscope with a 10x ocular lens. The white arrow indicates the perivitelline space, while the red arrow represents the relative position of the chorion. Ctrl: control; H-CDs: hydrothermal banana peel CDs; P-CDs: pyrolytic banana peel CDs. Scale bar 200 μm .

Evaluation of the acute toxic effects of banana peel carbon dots on zebrafish embryo survival

Malformations in zebrafish embryos were observed after 96 h of exposure (**Figure 5**). Notable malformations included eye malformations (eyepoint hypoplasia, asymmetrical eyes), pericardial edema, yolk sac malformations (edema, incomplete yolk sac depletion), tail malformations, and spinal curvature (scoliosis). The incidence of malformations increased in a concentration-dependent manner. At 2000 ppm, the highest frequency of malformations was observed with P-CDs, while H-CDs resulted in the highest frequency of malformations at 1000 and 2000 ppm (**Table 1**).

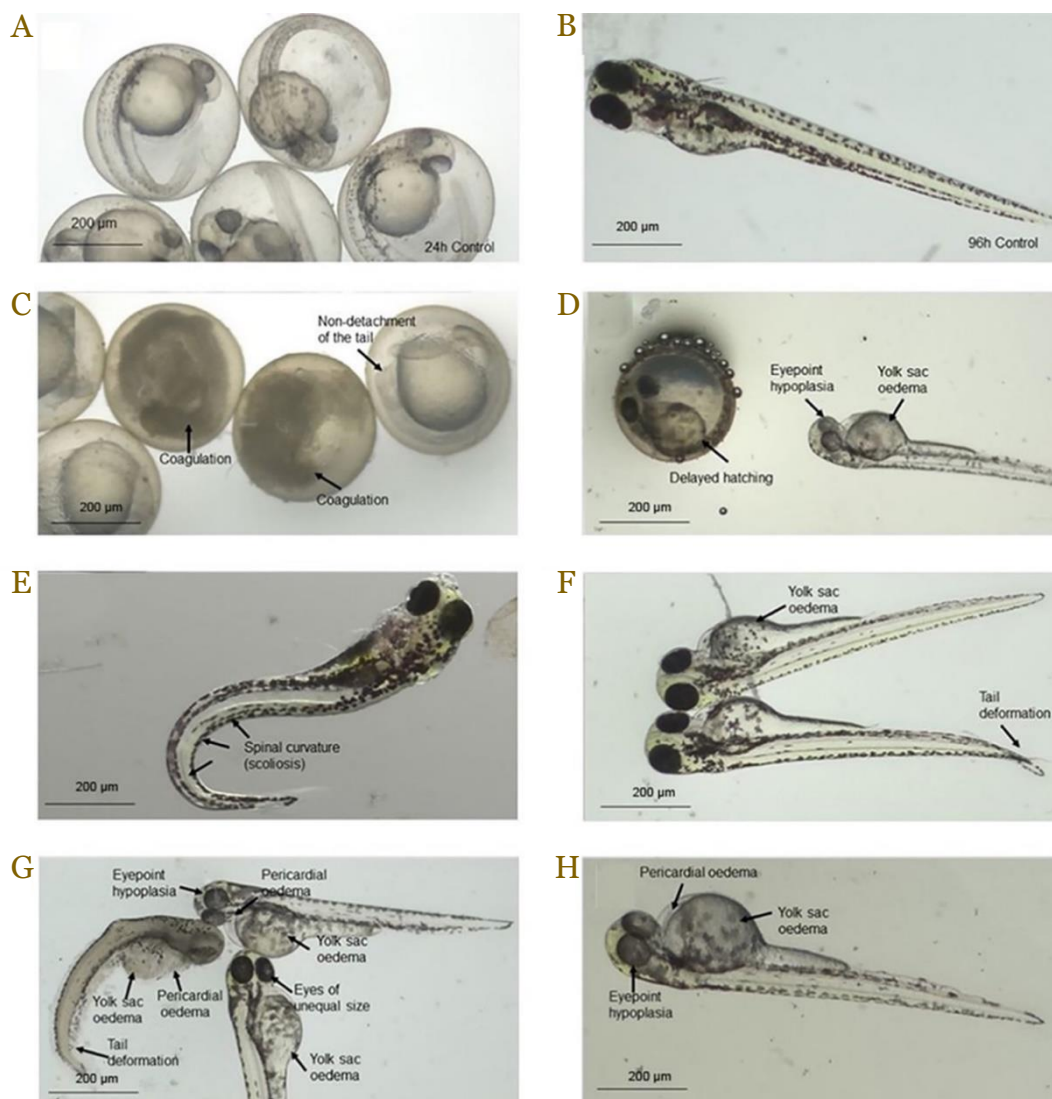


Figure 5. Representative images of zebrafish embryo malformations following exposure to banana peel carbon dots. Observations were made using a stereo microscope with a magnification of 1.575 \times , with a scale bar of 200 μm . Zebrafish embryos were exposed to the control E3 medium after (A) 24 h and (B) 96 h. (C) Coagulation of zebrafish embryos occurred following exposure to 1000 ppm hydrothermal banana peel carbon dots after 24 h. (D) Zebrafish exposed to 1000 ppm pyrolytic banana peel carbon dots after 96 h. (E) Zebrafish exposed to 250 ppm pyrolytic banana peel carbon dots after 96 h. (F) Zebrafish exposed to 500 ppm pyrolytic banana peel carbon dots after 96 h. Zebrafish exposed to (G) 500 ppm and (H) 2000 ppm hydrothermal banana peel carbon dots after 96 h.

Table 1. Embryotoxicity test of synthesized pyrolytic banana peel carbon dots (P-CDs) and hydrothermal banana peel carbon dots (H-CDs) using zebrafish animal test

Embryonic defects	P-CDs concentration (ppm)					H-CDs concentration (ppm)				
	125	250	500	1000	2000	125	250	500	1000	2000
Yolk sac edema	+	-	-	+	+	-	-	-	+	+
Yolk not depleted	-	-	-	+	+	-	-	-	+	+
Tail malformation	+	+	+	+	+	-	+	+	+	+
Pericardial edema	-	+	+	-	+	-	-	+	+	+
Spinal curvature (scoliosis)	-	-	+	+	+	-	-	-	+	+
Eye malformation	-	-	-	+	+	-	-	-	+	+

+ corresponds the presence of malformation

In addition to the observed malformations, the acute toxic effects were also reflected in survival and hatching rates. Zebrafish embryos were monitored for 120 h, with the number of

hatched and surviving embryos recorded and compared to the control and positive control groups (3,4-dichloroaniline). The survival rate of embryos decreased with increasing carbon dot concentration and prolonged exposure. For P-CDs, the survival rate was significantly lower compared to the control group ($p<0.05$), although exposure time did not significantly affect survival rates (Figure 6).

Similarly, for H-CDs, survival rates were significantly lower compared to the control group ($p<0.05$), with statistically significant differences ($p<0.05$) observed at 96 and 120 h of exposure. The hatching rates of both P-CDs and H-CDs at concentrations of 1000 and 2000 ppm were significantly different ($p<0.05$) from the control group (Figure 7). Both types of carbon dots showed significant differences ($p<0.05$) in hatching rates at 96 and 120 h of exposure.

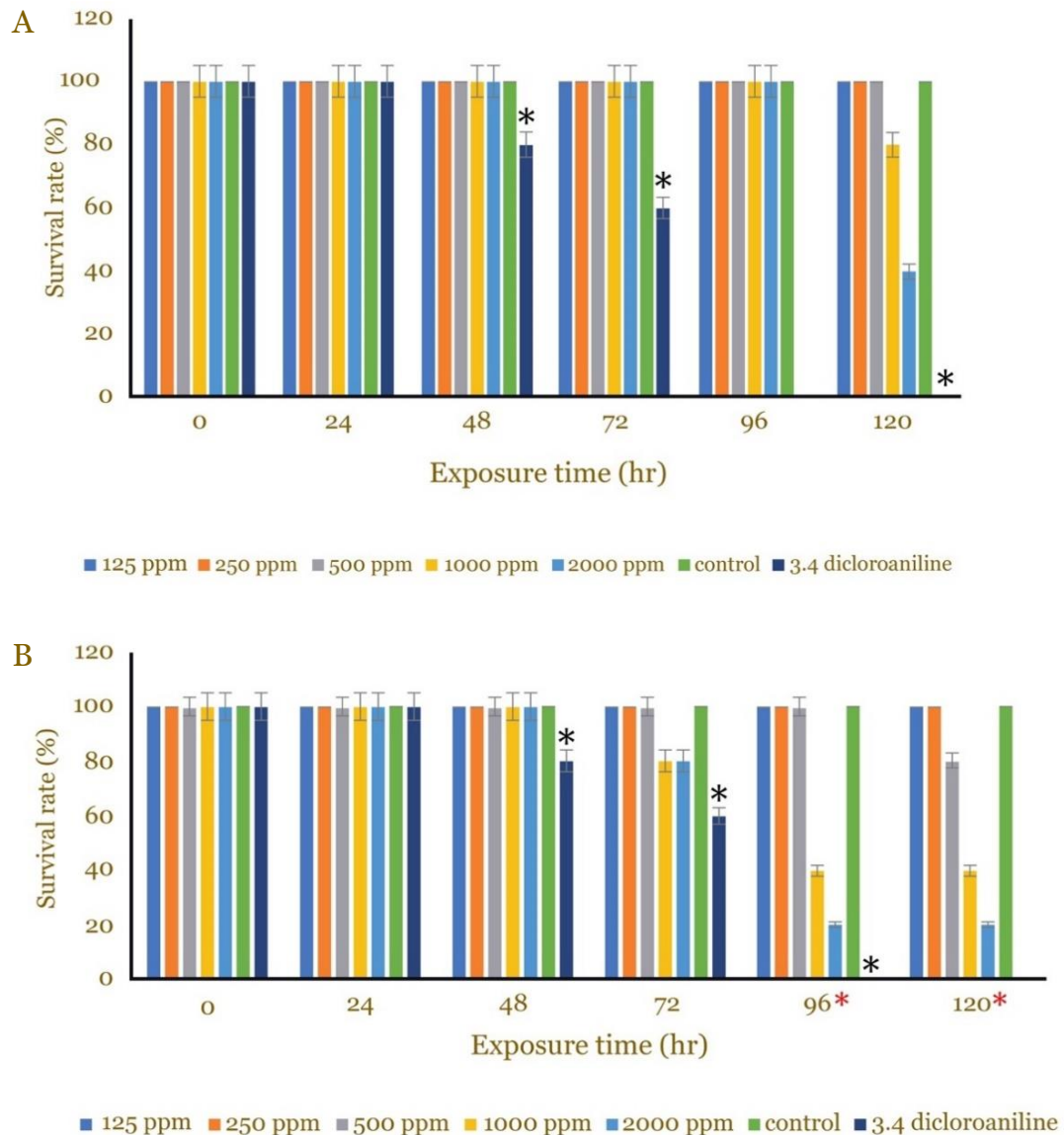


Figure 6. Survival rate of zebrafish following exposure to different concentrations of banana peel carbon dots. Survival rates of zebrafish embryos exposed to (A) pyrolytic banana peel carbon dots (P-CDs) and (B) hydrothermal banana peel carbon dots (H-CDs). Data are presented as mean±standard error (n=20 embryos). ANOVA followed by Tukey's test was performed. *Statistically significant at $p<0.05$ vs control; *Statistically significant at $p<0.05$ vs 0 hour.

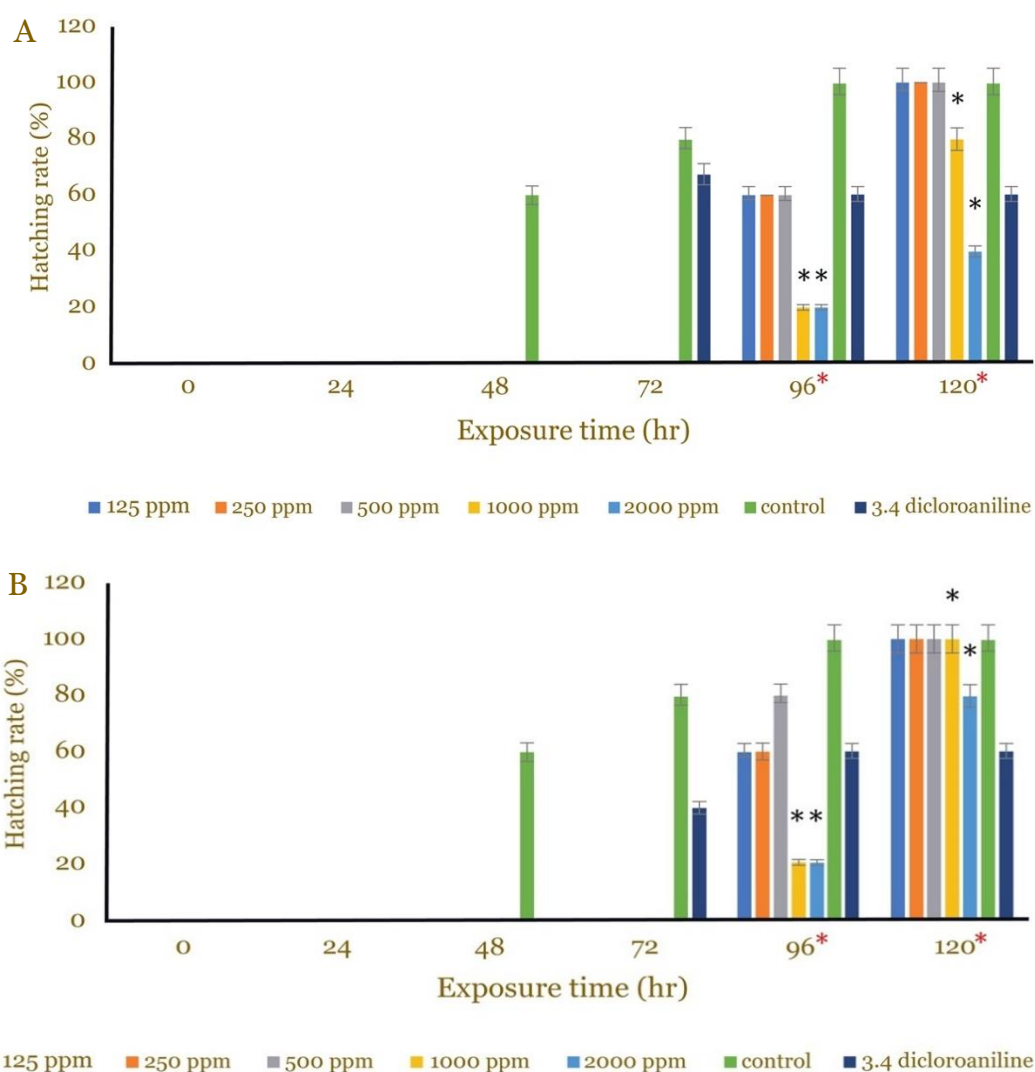


Figure 7. Hatching rate of zebrafish following exposure to different concentrations of banana peel carbon dots. Hatching rates of zebrafish embryos exposed to (A) pyrolytic banana peel carbon dots (P-CDs) and (B) hydrothermal banana peel carbon dots (H-CDs). Data are presented as mean±standard error (n=20 embryos). ANOVA followed by Tukey's test was performed. *Statistically significant at $p < 0.05$ vs control; **Statistically significant at $p < 0.05$ vs 0 hour.

Discussion

In the present study, banana peel carbon dots were synthesized using green synthesis methods: pyrolysis and hydrothermal techniques. These methods are cost-effective, simple, and produce high-quality carbon dots [22,28]. Pyrolysis involves the thermal decomposition of banana peel at elevated temperatures (300–800°C) in the absence of oxygen, while the hydrothermal technique involves reacting banana peel with water under high temperature and pressure (100–200°C, 1–2 MPa) [21,62]. Both methods were documented to be effective for producing carbon dots from banana peel and are environmentally sustainable [18,28,54]. Both methods are capable of producing carbon dots with particle sizes of less than 10 nm, with temperature, pressure, precursor, and time as variables that influence carbon dot size [63].

The characteristics of the carbon dots, including their optical properties, structure, and size, are influenced by the carbon source and synthesis conditions [21]. When using biomass as the carbon source, factors such as the type of biomass and specific hydrothermal conditions (time and temperature) impact the final structure of the carbon dots [9,21,23,28,52,64]. Banana peel carbon dots exhibit distinct physicochemical properties, including small particle sizes (below 10 nm), excellent optical behavior, and biochemical stability [18,28]. All carbon dots derived from

banana peels have a negative surface charge due to the presence of carboxyl and hydroxyl functional groups, which significantly affects their interactions with their surroundings [47].

The optical characteristics of natural carbon dots demonstrate a strong shift in absorption from the UV to the visible light spectrum [65]. The carbon core of the carbon dots exhibits two distinct absorption peaks. The primary peak at 230 nm results from the π - π^* transition within aromatic C-C bonds, while a secondary peak (shoulder) at 300 nm is attributed to n- π^* transitions in carbonyl (C=O) groups or other attached chemical groups [56,64,66-68]. Additionally, carbon dots synthesized from the same material but using various methods, such as ultrasonic, microwave, and hydrothermal techniques, display different absorption bands in the 250–300 nm range [69].

Zebrafish embryos and larvae are commonly used as model organisms to evaluate the efficacy of in vivo imaging techniques and to study the tissue distribution profiles of carbon dots [48,70,71]. The zebrafish model is approved for use in scientific research as per EU Directive 2010/63/EU [61]. In the present study, 125 ppm banana peel carbon dots were utilized for bioimaging by exposing zebrafish embryos (6 hpf) and larvae (84 hpf) to the carbon dots solution for 4 h. This concentration was chosen because it aligns with the developmental stages of zebrafish at this concentration of hydrothermal carbon dots, whereas the pyrolytic carbon dots at 125 ppm had minimal impact on embryo development. The present study indicates that carbon dots could be absorbed through the skin of zebrafish larvae, accumulating in the yolk sac, yolk extension, and eyes, suggesting a strong affinity for fatty substances. Fluorescent carbon dots can be valuable for studying fat transport and processing, with fluorescence intensity indicating tissue-specific binding [47]. The negative charge of the banana peel carbon dots may affect their fluorescence [72,73]. Comparative studies have shown that positively charged carbon dots exhibit stronger fluorescence signals under confocal microscopy, confirming that banana peel carbon dots generally exhibit moderate fluorescence due to their negative surface charge [34,43,72,73].

Fluorescence was not observed in the zebrafish embryo in the present study, indicating that the banana peel carbon dots cannot penetrate the embryos. A previous study suggested that short-term exposure to carbon dots does not result in long-term accumulation in zebrafish embryos, as they are eliminated through diffusion [34]. Additionally, the fish's digestive system can promptly eliminate carbon dots [38]. The presence of fluorescent signals in the chorion and perivitelline layers suggests that banana peel carbon dots can penetrate these regions, potentially impacting embryo development [37]. The chorion's pores, which are larger than the carbon dots, allow for their passage, with a size of 0.17 micrometers compared to the carbon dots' approximate diameter of 2-5 nanometers [43]. Surface functional groups such as -NH₂, -COOH, -CO, and -COH on carbon dots can interact selectively with biomolecules and binding sites in zebrafish, influencing fluorescence [38,64,67,74,75]. The functional group analysis of banana peel carbon dots using FTIR and their fluorescence properties suggest potential for bioimaging applications.

The toxicity of carbon dots was assessed based on malformations, survival, and hatching rates. In zebrafish, mortality with pyrolytic carbon dots occurred at concentrations of 1000 and 2000 ppm, with mortality rates of 20% and 60%, respectively, after 120 h of exposure. Hydrothermal carbon dots also caused mortality at 1000 and 2000 ppm, with rates of 20% at 72 hours and 60% and 80% at 96 and 120 h, respectively. Previous studies have reported varying mortality rates with different nanoparticles [37,40,42,52]. For instance, zinc oxide nanoparticles led to a 39% mortality rate at 10 ppm, while rutile-phase ZnO nanoparticles caused increased mortality at higher concentrations after a 96 h exposure period [42]. Carbon nanoparticles have also shown increased malformations and reduced hatching at concentrations of 50, 100, and 200 ppm from 4 to 96 hpf [35]. Non-doped, nitrogen-doped, and sulfur-doped carbon dots exhibited significant toxicity to zebrafish at concentrations exceeding 150 ppm [40,61]. Carbon dots with various surface functional groups (-CO-N(CH₃)₂, -COOH, and -NH₂) have demonstrated remarkable biocompatibility and low cytotoxicity [75]. Compared to other carbon nanoparticles, banana peel carbon dots exhibit lower toxicity to zebrafish.

The OECD #236 Fish Embryo Toxicity Test is effective for evaluating acute toxicity by monitoring zebrafish embryo development up to 96 hpf [37,57]. In this study, zebrafish embryos at 12 hpf were continuously exposed to banana peel carbon dots at concentrations ranging from 125 to 2000 ppm for 120 h. The test revealed that the LC₅₀ values for pyrolytic and hydrothermal

carbon dots were 1703.7 ppm and 933.2 ppm, respectively. Exposure to banana peel carbon dots at various concentrations significantly impacted zebrafish embryo maturation, causing slower hatching and development compared to the control group. The treated group exhibited birth defects that became more severe with increased exposure duration and concentration.

A previous study indicated that fruit-based carbon dots, such as those derived from kiwi, pear, and avocado, can cause developmental toxicity in zebrafish, characterized by yolk sac edema, eye abnormalities, and reduced hatching rates [47]. Consistent with these findings, the present study observed abnormalities in the yolk sac, which could disrupt nutrient intake and negatively affect embryo growth. The yolk sac provides essential nutrients for embryo development, and damage to this structure can lead to abnormal growth due to nutrient deficiencies [35,50].

Abnormal spinal curvature, potentially caused by scoliosis or notochord issues, was another observed physical change, affecting the embryo's movement and coordination [35]. Additionally, pericardial edema and eye malformations were noted. Previous studies have found that carbon nanoparticles can cause ultrastructural changes in heart tissue and impact visual development [35,36,50].

The summarized findings indicate that banana peel carbon dots exhibit relatively high toxicity thresholds compared to other carbon nanoparticles (**Table 2**), making them promising for medical applications such as labeling biological materials, drug delivery, and cancer treatment. However, before its widespread use, to accurately assess the toxic effects on zebrafish embryo development, it is recommended to use embryos at the youngest possible age (around 4 hpf) [35,50]. In this study, embryos aged 12 hpf were utilized due to limitations in observing the timing of fish mating that occurred at night towards dawn. To support the toxicity data from banana peel carbon dots, research should be continued in studies using rats to ensure a comprehensive assessment of the toxicity profile.

Table 2. Toxicity assessment results of various carbon dots in zebrafish

Carbon dots (CDs) particle	Raw materials	Particle size (nm)	LC ₅₀ (ppm)	References
Kiwi-CDs	Kiwi fruits	4.35±0.04	1444	[47]
Pear-CDs	Pear fruits	4.12±0.03	2224	[47]
Avocado-CDs	Avocado fruits	4.42±0.05	1964	[47]
Black pepper-CDs	Black pepper	N/A	985	[47]
N,S-doped CQDs	Citric acid	8	149.92	[40]
N-doped CQDs	Citric acid	2.5	399.95	[40]
Non-doped CQDs	Citric acid	4	548.48	[40]
Babassu coconut CDs	Babassu coconut mesocarp	19.8	>1000	[52]
CQDac	Ammonium citrate	4.1±1.20	500	[34]
CQDspd	Spermidine	6.3±1.35	100	[34]
Banana peel P-CDs	Banana peel	1.8±0.4	1703.7	The present study
Banana peel H-CDs	Banana peel	5.4±1.3	933.2	The present study

CQDac: carbon quantum dots derived ammonium citrate; CQDs: carbon quantum dots; CQDspd: carbon quantum dots derived spermidine; H-CDs: hydrothermal banana peel carbon dots; LC₅₀: lethal concentration; P-CDs: pyrolysis-banana peel carbon dots.

Conclusion

Banana peel-derived carbon dots demonstrated substantial green fluorescence across various anatomical regions of zebrafish, including the eye, lens, yolk sac, intestine, and tail. The intense fluorescence observed around the yolk sac, particularly near the intestine, indicates their potential utility in studying fat transport and processing within zebrafish embryos. Additionally, the strong fluorescent signals in the eyes and melanophore stripes suggest a high affinity for melanin, highlighting their potential for investigating melanin-rich areas in zebrafish larvae. Toxicity assessments revealed that carbon dots synthesized via the pyrolysis method exhibited lower toxicity (LC₅₀ of 1707.3 ppm) compared to those synthesized via the hydrothermal method (LC₅₀ of 993 ppm). These LC₅₀ values underscore the non-toxic nature of the synthesized carbon dots and suggest their promising potential for biomedical applications in zebrafish studies.

Ethics approval

Ethical clearance for the present study was obtained from Ethical Committee for Animal Research, Universitas Airlangga (Approval number: 784/HRECC.FODM/X/2022).

Acknowledgments

The researchers extend their deepest gratitude to the ITB Olympus Bioimaging Center (IOBC); the Study Program of E2M Laboratory, Faculty of Mathematics and Science, Bandung Institute of Technology; and the Laboratory of Development Animals and Space Optics, School of Science and Technology, Bandung Institute of Technology. Their support and collaboration have been invaluable.

Competing interests

All the authors declare that there are no conflicts of interest.

Funding

The present study was supported by Beasiswa Pendidikan Indonesia (Grant number: 202101120930), the Center for Higher Education Fund (BPPT), the Ministry of Education, Culture, Research, and Technology, and the Indonesia Endowment Fund for Education Agency (LPDP), Ministry of Finance, Indonesia.

Underlying data

Derived data supporting the findings of this study are available from the corresponding author on request.

How to cite

Wijayanti NPAD, Permatasari FA, Damayanti S, *et al.* Toxicity assessment and bioimaging potential of carbon dots synthesized from banana peel in zebrafish model. *Narra J* 2024; 4 (3): e1228 - <http://doi.org/10.52225/narra.v4i3.1228>.

Reference

1. Fibriani A, Taharuddin AAP, Yamahoki N, *et al.* Porphyrin-derived carbon dots for an enhanced antiviral activity targeting the CTD of SARS-CoV-2 nucleocapsid. *J Genet Eng Biotechnol* 2023;21(1):93.
2. Fibriani A, Taharuddin AAP, Stephanie R, *et al.* Curcumin-derived carbon-dots as a potential COVID-19 antiviral drug. *Heliyon* 2023;9(9):e20089.
3. Mailisa W, Annisa WD, Permatasari FA, *et al.* In Vitro and silico studies on the N-doped carbon dots potential in ACE2 expression modulation. *ACS Omega* 2023;8(11):10077-10085.
4. Santika AS, Permatasari FA, Umami R, *et al.* Revealing the synergetic interaction between amino and carbonyl functional groups and their effect on the electronic and optical properties of carbon dots. *Phys Chem Chem Phys* 2022;24(44):27163-27172.
5. Permatasari FA, Umami R, Sundari CDD, *et al.* New insight into pyrrolic-N site effect towards the first NIR window absorption of pyrrolic-N-rich carbon dots. *Nano Res* 2023;16(4):6001-6009.
6. Umami R, Permatasari FA, Muyassiroh DAM, *et al.* A rational design of carbon dots via the combination of nitrogen and oxygen functional groups towards the first NIR window absorption. *J Mater Chem C Mater* 2022;10(4):1394-1402.
7. Peng Z, Han X, Li S, *et al.* Carbon dots: Biomacromolecule interaction, bioimaging and nanomedicine. *Coord Chem Rev* 2017;343:256-277.
8. Boakye-Yiadom KO, Kesse S, Opoku-Damoah Y, *et al.* Carbon dots: Applications in bioimaging and theranostics. *Int J Pharm* 2019;564:308-317.
9. Ray SC, Saha A, Jana NR, *et al.* Fluorescent carbon nanoparticles: Synthesis, characterization, and bioimaging application. *J Phys Chem C* 2009;113(43).
10. Shen CL, Liu HR, Lou Q, *et al.* Recent progress of carbon dots in targeted bioimaging and cancer therapy. *Theranostics* 2022;12(6):2860-2893.
11. Li X, Zhao S, Li B, *et al.* Advances and perspectives in carbon dot-based fluorescent probes: Mechanism, and application. *Coord Chem Rev* 2021;431:213686.

12. Lin X, Xiong M, Zhang J, *et al.* Carbon dots based on natural resources: Synthesis and applications in sensors. *Microchem J* 2021;160:105604.
13. Ross S, Wu RS, Wei SC, *et al.* The analytical and biomedical applications of carbon dots and their future theranostic potential: A review. *J Food Drug Anal* 2020;28(4):678-696.
14. Yuan Y, Guo B, Hao L, *et al.* Doxorubicin-loaded environmentally friendly carbon dots as a novel drug delivery system for nucleus targeted cancer therapy. *Colloids Surf B Biointerfaces* 2017;159:349-359.
15. Lin CJ, Chang L, Chu HW, *et al.* High amplification of the antiviral activity of curcumin through transformation into carbon quantum dots. *Small* 2019;15(41):e1902641.
16. Zhang W, Ma R, Gu S, *et al.* Nitrogen and phosphorus co-doped carbon dots as an effective fluorescence probe for the detection of doxorubicin and cell imaging. *Opt Mater* 2022;128:112323.
17. He L, Wang T, An J, *et al.* Carbon nanodots zeolitic imidazolate framework-8 nanoparticles for simultaneous pH-responsive drug delivery and fluorescence imaging. *CrystEngComm* 2014;16(16):3259.
18. Atchudan R, Jebakumar IETN, Shanmugam M, *et al.* Sustainable synthesis of carbon quantum dots from banana peel waste using hydrothermal process for in vivo bioimaging. *Physica E Low Dimens Syst Nanostruct* 2021;126:114417.
19. Li Z, Wang Q, Zhou Z, *et al.* Green synthesis of carbon quantum dots from corn stalk shell by hydrothermal approach in near-critical water and applications in detecting and bioimaging. *Microchem J* 2021;166:106250.
20. Huang Q, Hu S, Zhang H, *et al.* Carbon dots and chitosan composite film based biosensor for the sensitive and selective determination of dopamine. *Analyst* 2013;138(18):5417-5423.
21. Ozyurt D, Kobaisi M Al, Hocking RK, *et al.* Properties, synthesis, and applications of carbon dots: A review. *Carbon Trends* 2023;12:100276.
22. Kurian M, Paul A. Recent trends in the use of green sources for carbon dot synthesis—A short review. *Carbon Trends* 2021;3:100032.
23. Liu ML, Chen BB, Li CM, *et al.* Carbon dots: Synthesis, formation mechanism, fluorescence origin and sensing applications. *Green Chem* 2019;21(3):449-471.
24. Thakur N, Manna P, Das J. Synthesis and biomedical applications of nanoceria, a redox active nanoparticle. *J Nanobiotechnology* 2019;17(1):84.
25. Sharma A, Das J. Small molecules derived carbon dots: synthesis and applications in sensing, catalysis, imaging, and biomedicine. *J Nanobiotechnology* 2019;17(1):92.
26. Atchudan R, Edison TNJI, Perumal S, *et al.* Hydrophilic nitrogen-doped carbon dots from biowaste using dwarf banana peel for environmental and biological applications. *Fuel* 2020;275:117821.
27. Atchudan R, Edison TNJI, Aseer KR, *et al.* Hydrothermal conversion of *Magnolia liliiflora* into nitrogen-doped carbon dots as an effective turn-off fluorescence sensing, multi-colour cell imaging and fluorescent ink. *Colloids Surf B Biointerfaces* 2018;169:321-328.
28. Nguyen TN, Le PA, Phung VBT. Facile green synthesis of carbon quantum dots and biomass-derived activated carbon from banana peels: Synthesis and investigation. *Biomass Convers Biorefin* 2022;12(7):2407-2416
29. Bandi R, Gangapuram BR, Dadigala R, *et al.* Facile and green synthesis of fluorescent carbon dots from onion waste and their potential applications as sensor and multicolour imaging agents. *RSC Adv* 2016;6(34):28633-28639.
30. de Oliveira BP, da Silva Abreu FOM. Carbon quantum dots synthesis from waste and by-products: Perspectives and challenges. *Mater Lett* 2021;282:128764.
31. Himaja AL, Karthik PS, Sreedhar B, *et al.* Synthesis of carbon dots from kitchen waste: Conversion of waste to value added product. *J Fluoresc* 2014;24(6):1767-1773.
32. Fan H, Zhang M, Bhandari B, *et al.* Food waste as a carbon source in carbon quantum dots technology and their applications in food safety detection. *Trends Food Sci Technol* 2020;95:86-96.
33. von Helffeld R, Brotzmann K, Baumann L, *et al.* Adverse effects in the fish embryo acute toxicity (FET) test: A catalogue of unspecific morphological changes versus more specific effects in zebrafish (*Danio rerio*) embryos. *Environ Sci Eur* 2020;32(1):122.
34. Chung CY, Chen YJ, Kang CH, *et al.* Toxic or not toxic, that is the carbon quantum dot's question: A comprehensive evaluation with zebrafish embryo, eleutheroembryo, and adult models. *Polymers* 2021;13(10):1598.
35. Shi L, Qian Y, Shen Q, *et al.* The developmental toxicity and transcriptome analyses of zebrafish (*Danio rerio*) embryos exposed to carbon nanoparticles. *Ecotoxicol Environ Saf* 2022;234:113417.
36. Ghobadian M, Nabiuni M, Parivar K, *et al.* Toxic effects of magnesium oxide nanoparticles on early developmental and larval stages of zebrafish (*Danio rerio*). *Ecotoxicol Environ Saf* 2015;122:260-267.

37. Dumitrescu E, Wallace K, Andreescu S. Nanotoxicity assessment using embryonic zebrafish. *Methods Mol Biol* 2019;1894:331-343.
38. Khajuria DK, Kumar VB, Karasik D, *et al.* Fluorescent nanoparticles with tissue-dependent affinity for live zebrafish imaging. *ACS Appl Mater Interfaces* 2017;9(22):18557-18565.
39. D'Costa A, Shepherd IT. Zebrafish development and genetics: Introducing undergraduates to developmental biology and genetics in a large introductory laboratory class. *Zebrafish* 2009;6(2):169-177.
40. Chousidis I, Stalikas CD, Leonardos ID. Induced toxicity in early-life stage zebrafish (*Danio rerio*) and its behavioral analysis after exposure to non-doped, nitrogen-doped and nitrogen, sulfur-co doped carbon quantum dots. *Environ Toxicol Pharmacol* 2020;79:103426.
41. Liu X, Dumitrescu E, Kumar A, *et al.* Differential lethal and sublethal effects in embryonic zebrafish exposed to different sizes of silver nanoparticles. *Environ Pollut* 2019;248:627-634.
42. Sezer S, Yücel A, Özhan Turhan D, *et al.* Comparison of ZnO doped different phases TiO₂ nanoparticles in terms of toxicity using zebrafish (*Danio rerio*). *Chemosphere* 2023;325:138342.
43. Liu H, Wang X, Wu Y, *et al.* Toxicity responses of different organs of zebrafish (*Danio rerio*) to silver nanoparticles with different particle sizes and surface coatings. *Environ Pollut* 2019;246:414-422.
44. Verma SK, Nisha K, Panda PK, *et al.* Green synthesized MgO nanoparticles infer biocompatibility by reducing in vivo molecular nanotoxicity in embryonic zebrafish through arginine interaction elicited apoptosis. *Sci Total Environ* 2020;713:136521.
45. Lin HY, Yen SC, Kang CH, *et al.* How to evaluate the potential toxicity of therapeutic carbon nanomaterials? A comprehensive study of carbonized nanogels with multiple animal toxicity test models. *J Hazard Mater* 2022;429:128337.
46. Abramenko NB, Demidova TB, Abkhalimov EV, *et al.* Ecotoxicity of different-shaped silver nanoparticles: Case of zebrafish embryos. *J Hazard Mater* 2018;347:89-94.
47. Dias C, Vasimalai N, P. Sárria M, *et al.* Biocompatibility and bioimaging potential of fruit-based carbon dots. *Nanomaterials* 2019;9(2):199.
48. Umar E, Ikram M, Haider J, *et al.* A state-of-the-art review on carbon quantum dots: Prospective, advances, zebrafish biocompatibility and bioimaging in vivo and bibliometric analysis. *Sustain Mater Technol* 2023;35:e00529.
49. Massarsky A, Dupuis L, Taylor J, *et al.* Assessment of nanosilver toxicity during zebrafish (*Danio rerio*) development. *Chemosphere* 2013;92(1):59-66.
50. Dumitrescu E, Karunaratne DP, Prochaska MK, *et al.* Developmental toxicity of glycine-coated silica nanoparticles in embryonic zebrafish. *Environ Pollut* 2017;229:439-447.
51. Jafari A, Rashidipour M, Kamarehi B, *et al.* Toxicity of green synthesized TiO₂ nanoparticles (TiO₂ NPs) on zebrafish. *Environ Res* 2022;212:113542.
52. Costa RS, de Castro MO, da Silva GH, *et al.* Carbon-dots from babassu coconut (*Orbignya speciosa*) biomass: Synthesis, characterization, and toxicity to *Daphnia magna*. *Carbon Trends* 2021;5:100133.
53. Rajesh TP, Balaji R, Chen SM, *et al.* The iron oxide/polymer nanocomposites for targeted drug delivery and toxicity investigation on zebrafish (*Danio rerio*). *Inorg Chem Commun* 2021;125:108447.
54. Sigiro M. Natural biowaste of banana peel-derived porous carbon for in-vitro antibacterial activity toward *Escherichia coli*. *Ain Shams Eng J* 2021;12(4):4157-4165.
55. Vandarkuzhali SAA, Jeyalakshmi V, Sivaraman G, *et al.* Highly fluorescent carbon dots from Pseudo-stem of banana plant: Applications as nanosensor and bio-imaging agents. *Sens Actuators B Chem* 2017;252:894-900.
56. De B, Karak N. A green and facile approach for the synthesis of water soluble fluorescent carbon dots from banana juice. *RSC Adv* 2013;3(22):8286.
57. OECD. OECD guideline for the testing of chemicals: Fish embryo acute aquatic toxicity (FET) test, 2013. Available from: https://www.oecd-ilibrary.org/environment/test-no-236-fish-embryo-acute-toxicity-fet-test_9789264203709-en. Accessed: 17 July 2023.
58. Flinney DJ. Probit analysis (2nd ed). *J Inst Actuar* 1952;78(3):388-390.
59. Fernandes IM, Bastos YF, Barreto DS, *et al.* The efficacy of clove oil as an anaesthetic and in euthanasia procedure for small-sized tropical fishes. *Braz J Biol* 2017;77(3):444-450.
60. Strykowski JL, Schech JM. Effectiveness of recommended euthanasia methods in larval zebrafish (*Danio rerio*). *J Am Assoc Lab Anim Sci* 2015;54(1):81-84.

61. European Union. Directive 2010/63/EU of the European parliament and of the council of 22 september 2010 on the protection of animals used for scientific purposes. Available from: <https://eur-lex.europa.eu/eli/dir/2010/63/oj>. Accessed: 22 July 2023.
62. Aji MP, Susanto, Wiguna PA, *et al.* Facile synthesis of luminescent carbon dots from mangosteen peel by pyrolysis method. *J Theor Appl Phys* 2017;11(2):119-126.
63. Vibhute A, Patil T, Gambhir R, *et al.* Fluorescent carbon quantum dots: Synthesis methods, functionalization and biomedical applications. *Appl Surf Sci Adv* 2022;11:100311.
64. Wang R, Lu KQ, Tang ZR, *et al.* Recent progress in carbon quantum dots: Synthesis, properties and applications in photocatalysis. *J Mater Chem A Mater* 2017;5(8):3717-3734.
65. Nair A, Haponiuk JT, Thomas S, *et al.* Natural carbon-based quantum dots and their applications in drug delivery: A review. *Biomed Pharmacother* 2020;132:110834.
66. Wang D, Wang Z, Zhan Q, *et al.* Facile and scalable preparation of fluorescent carbon dots for multifunctional applications. *Engineering* 2017;3(3):402-408.
67. Wang B, Song H, Qu X, *et al.* Carbon dots as a new class of nanomedicines: Opportunities and challenges. *Coord Chem Rev* 2021;442:214010.
68. Wang CI, Wu WC, Periasamy AP, *et al.* Electrochemical synthesis of photoluminescent carbon nanodots from glycine for highly sensitive detection of hemoglobin. *Green Chem* 2014;16(5):2509-2514.
69. Mishra V, Patil A, Thakur S, *et al.* Carbon dots: Emerging theranostic nanoarchitectures. *Drug Discov Today* 2018;23(6):1219-1232.
70. Jana P, Dev A. Carbon quantum dots: A promising nanocarrier for bioimaging and drug delivery in cancer. *Mater Today Commun* 2022;32:104068.
71. Kang YF, Li YH, Fang YW, *et al.* Carbon quantum dots for zebrafish fluorescence imaging. *Sci Rep* 2015;5(1):11835.
72. Usman M, Zaheer Y, Younis MR, *et al.* The effect of surface charge on cellular uptake and inflammatory behavior of carbon dots. *Colloid Interface Sci Commun* 2020;35:100243.
73. Geys J, Nemmar A, Verbeken E, *et al.* Acute toxicity and prothrombotic effects of quantum dots: Impact of surface charge. *Environ Health Perspect* 2008;116(12):1607-1613.
74. Yang ST, Cao L, Luo PG, *et al.* Carbon dots for optical imaging in vivo NIH public access. *J Am Chem Soc* 2009;131(32):11308-11309.
75. Liang W, Li Z, Li H, *et al.* The influence of functional group on photoluminescence properties of carbon dots. *ECS J Solid State Sci Technol* 2019;8(12):R176-R182.